

Photochemistry on surfaces

D. Oelkrug, W. Flemming, R. Füllemann, R. Günther,
W. Honnen, G. Krabichler, M. Schäfer, S. Uhl

Physikalische und Theoretische Chemie, Universität D-7400 Tübingen, FRG

Abstract - The photophysics and photochemistry of organic molecules (aromatics, aza-aromatics, diphenylpolyenes, azobenzene, triphenylmethane dyes, thioindigo) adsorbed on metal oxides (alumina, silica, thoria, titania) were investigated by steady-state and time-resolved diffuse reflectance and luminescence spectroscopy.

The fluorescence decay curves of almost all adsorbates are non-exponential. This effect is discussed in terms of different polarizing surface sites, aggregation, and interference between directly emitted and scattered fluorescence radiation.

A method is elaborated to determine rate constants and quantum yields of photoreactions in strongly scattering rigid media by photometric measurements using the model of radiative transfer. The method is applied to quantify internal and translational mobilities of adsorbed photoexcited molecules, ring closure reactions, bimolecular photoprocesses, and charge transfer between the adsorbent and the adsorbate.

INTRODUCTION

Photochemical reactions are conventionally studied in homogeneous phases and, as far as possible, in ideally stirred media. These conditions, however, are not to be realized in many systems of biological or technical interest. The medium can be strongly light-scattering and highly viscous, and the reacting species can be very inhomogeneously distributed in it (e.g. in membranes or in the adsorbed state). Compared with the total activities in photochemical research, the heterogeneous phenomena have received up to now only moderate attention. But the attention is strongly growing - see international meetings (ref. 1-4) - and the fields of artificial photosynthesis, photocatalysis, photochemistry of adsorbed molecules, or photochemistry at electrode/electrolyte interfaces become more and more attractive.

In this paper a review will be given of our recent work on the photophysics and photochemistry of molecules adsorbed on metal oxides. The main fields to which we would like to contribute are 1) the electronic structures and excited state lifetimes of adsorbates, 2) the internal mobility of photoexcited adsorbates, 3) the translational mobility and bimolecular photoreactions of adsorbates, 4) the electron and proton transfer in the photoexcited adsorbate/adsorbent system, 5) the quantitative description of photochemical conversions in strongly scattering media, including the photometric determination of quantum yields and rate constants.

Preferably those experimental techniques should be applied in surface photochemistry which avoid any desorption of the reactants. A combination of luminescence and electronic absorption spectroscopy - the latter in the diffuse reflectance mode - has proved to be a sensitive and selective tool to analyze the components and kinetics of photoreactions on polycrystalline solids. In the stationary version (ref. 5-8), adsorbates at coverages of fractions down to 10^{-5} or 10^{-6} of a monolayer can be characterized, providing the adsorbates are strongly luminescent. In the time-resolved luminescence version (ref. 9-14) and diffuse reflectance absorption version (ref. 15-17), the lifetimes of excited states, photochemical intermediates, rearrangement and diffusion processes in the picosecond to second timescale, as well as surface inhomogeneities can be studied.

The preparation and pretreatment of the adsorbents are very crucial parameters for the chemical activity of the surfaces. Without pretreatment, the surfaces of metal oxides are completely covered with hydroxyl groups and additional physisorbed water. The physisorbed water is desorbed by heating the adsorbents to roughly $T_a = 100$ °C. By further heating the remaining hydroxyl layer is also desorbed as water, leaving back vicinal and isolated

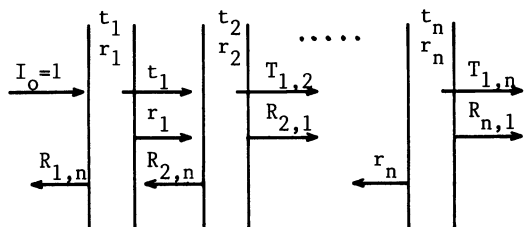
hydroxyl groups, highly strained Me-O-Me bonds (e.g. on silica), or single-centered oxygen ions and coordinatively unsaturated metal ions (e.g. on alumina). The process of dehydroxylation takes place over a very large temperature range from ca. 100 °C to 1000 °C. The different stages of dehydration can be monitored very precisely by flourescent bases and acids like acridine or 9-anthroic acid acting as sensitive probes for Broensted acidity and basicity of the surfaces (ref. 18). The dehydroxylation can be monitored by flourescent aromatic hydrocarbons forming EDA-complexes or radical pairs with coordinatively unsaturated metal ions (ref. 7,19).

The picture of the partly hydrated surface of a polycrystalline oxide has to be completed by surface irregularities (point defects, dislocations, micropores) which are particularly polarizing sites for the electronic system of the adsorbates or are favouring their aggregation. Highly porous oxides are preferently obtained by hydrolysis of suitable compounds in aqueous media and following thermal treatment. Non porous spherical particles with diameters down to ca. 5 nm are obtained by thermal hydrolysis in the gas phase (aerosols). The two types of adsorbents have a quite different effect on the chemical nature of the adsorbates.

Finally, the technique of adsorption is very important for the structures and subsequent chemical reactions of the adsorbates. From the thermodynamic point of view the adsorption under equilibrium conditions, e.g. from liquid solutions, is to be preferred. However, the surface can be modified by the solvent or traces of water in it, especially if it was pretreated at higher temperatures. It is also quite difficult to distinguish between reactions taking place exclusively at the surface or under participation of the liquid phase. The solvent is therefore very often evaporated off prior to the photochemical investigation. However, this procedure has some solid/liquid chromatographic effect and favours the aggregation of the adsorbates (ref. 6,20,21) far beyond monomolecular coverage. It favours also precipitation in those cases where the adsorption-desorption equilibrium is not distinctly shifted to the adsorbed state. The disadvantages of the liquid phase technique can be avoided by adsorption from the gas phase under high vacuum conditions. This method is preferred in our laboratory and can be applied to non polar adsorptives with masses up to e.g. coronene (ref. 22) and to polar adsorptives with slightly smaller masses. Of course, the method fails mostly to work with ionic compounds.

PHOTOMETRIC EVALUATION OF PHOTOREACTIONS IN LIGHT-SCATTERING RIGID MEDIA

Reactions on a single plane surface of a non absorbing solid are most easily evaluable theoretically, but most difficultly to be followed photometrically. Even at monolayer coverage (molecular distance ca. 10^{-7} cm) and reasonable molecular absorption cross sections of 10^{-16} cm² ($\epsilon \approx 6 \times 10^4$ M⁻¹cm⁻¹) the absorbed part of the incident light is only about 1 %. Both the reflection r and the transmittance t at the phase boundary are reduced by this amount. In significant experiments the coverage of the surface should not exceed the fraction of 0.01 to 0.1 of a monolayer, in order to separate distinctly between adsorbate-adsorbent and adsorbate-adsorbate interactions. Then the measurable optical quantities are correspondingly smaller. The amount of absorption and the change of reflection can be enlarged by putting many slices of the solid in series, each covered with the adsorbate. The intensities of the transmitted and reflected light can then be calculated at any point of the system using the following recursion formulae



$$R_{1,n+1} = R_{1,n} + \frac{r_{n+1} T_{1,n}^2}{1 - r_{n+1} R_{1,n}}$$

$$T_{1,n+1} = \frac{t_{n+1} T_{1,n}}{1 - r_{n+1} R_{n,1}}$$

With the same formulae the local intensity changes and local conversion rates during a photochemical reaction as well as the changes of the total reflection ΔR and total transmittance ΔT of the sample can be calculated. The latter quantities are directly comparable with the experiment.

Most of the realistic systems will not consist of an ensemble of plane parallel slices but of a large number of disordered microcrystals. In principal the calculation procedure of the above equations can be maintained by formally cutting the sample into very thin (approx. differential) slices parallel to the macroscopic surface. In detail some modifications have to be considered: Specular reflection at the phase boundaries has to be replaced by scattering at the densely packed microcrystals. The differential scattering process can be appro-

ximately treated as isotropic. The total reflection of the sample has to be replaced by diffuse reflectance. The photon density B (mol photons per unit volume) inside the sample depends not only on the optical constants but also on the geometry of irradiation.

An example for incident radiation parallel to the normal of the macroscopic surface ($\theta_0 = 0^\circ$) is given in Fig. 1. The incident radiation is attenuated by $B_{inc} = B_0 \exp(-(\alpha + \sigma)x/\cos\theta_0)$, where x is the local coordinate inside the sample with the illuminated surface at $x = 0$, α is the absorption coefficient per unit length, similar to that of the Lambert-Beer law, and σ is the scattering coefficient. It defines any part of the radiation scattered per unit length out from its original direction.

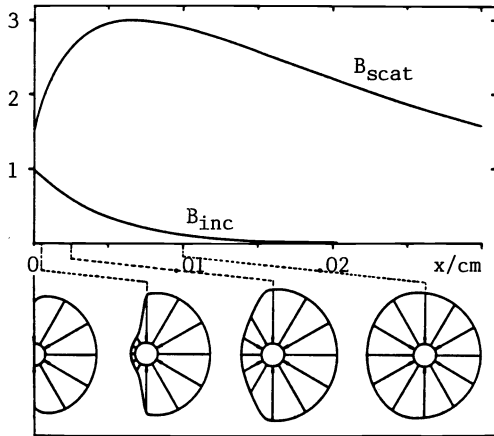


Fig. 1. Local and angular distribution of the photon density B inside a semi-infinite scattering and absorbing sample. The contributions of the incident and scattered parts are given separately.

Density of irradiation $B_0 = 1$
 Angle of irradiation $\theta_0 = 0^\circ$
 Absorption coefficient $\alpha = 2 \text{ cm}^{-1}$
 Scattering coefficient $\sigma = 200 \text{ cm}^{-1}$

The scattered part B_{scat} of the photon density, integrated over the whole solid angle, first increases with x and then decreases approximately by an exponential function. The angular distribution of B_{scat} is strongly dependent on x in the regions near the illuminated surface, it becomes constant in the deeper parts of the sample. Both the x - and θ -dependences of B_{scat} were calculated by Chandrasekhar's model of radiative transfer in semi-infinite layers (ref. 23).

Under diffuse incident irradiation the maximum in B_{scat} disappears and the angular distribution becomes only very little dependent on x . In this case simpler approximations of the equation of radiative transfer like e.g. the Kubelka-Munk model (ref. 24) can be applied to calculate the progress of a photochemical reaction. An example of irreversible photobleaching is given in Fig.2. Contrary to Fig.1 a strongly absorbing sample has been chosen. The absorber A is embedded in or adsorbed on a non-absorbing scatterer.

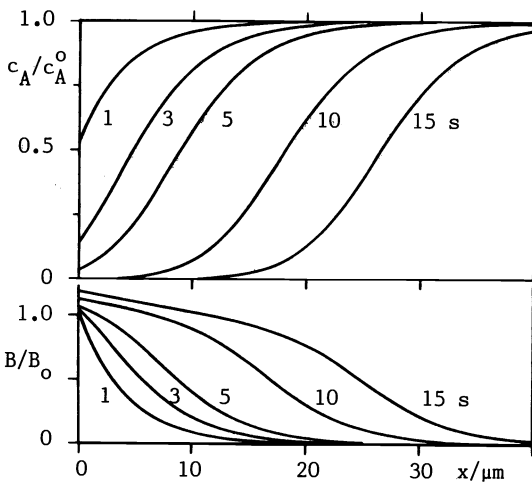


Fig. 2. Photobleaching $A \rightarrow B$ of a strongly absorbing, scattering sample under diffused incident irradiation.

$I_0 = 2 \cdot 10^{-9} \text{ Einstein cm}^{-2} \text{ s}^{-1}$

Concentration and photon density profiles at different irradiation times are calculated by numerical integration of the Kubelka-Munk equations. The diffuse reflectance is obtained by

$$R(t) = \frac{B(t, x=0)}{B_0} - 1$$

$\alpha = 2300 \text{ cm}^{-1}, \sigma = 330 \text{ cm}^{-1}$

During the reproduced time of reaction only a very thin layer of ca. 30 μm is bleached on top of unbleached material. The reflectance, however, has changed by an appreciable amount from $R = 0.02$ to $R = 0.28$. This demonstrates that typically small conversions will produce large reflectance changes in scattering and rigid systems.

Two experimental examples will be shortly discussed to give an idea about the applicability of the method. The first (Fig. 3) stands for an almost reversible trans - cis photoisomerization with wavelength dependent quantum yields and adsorbate coverages to give medium absorbing samples. The second (Fig. 4) stands for a photoreduction catalyzed by titania. Both α and σ of the second sample are much higher than of the first one. Thus the reaction takes place in a very small region near the illuminated macroscopic surface and, despite of a rather low photochemical quantum yield, the photometric trace is much steeper than in the first example.

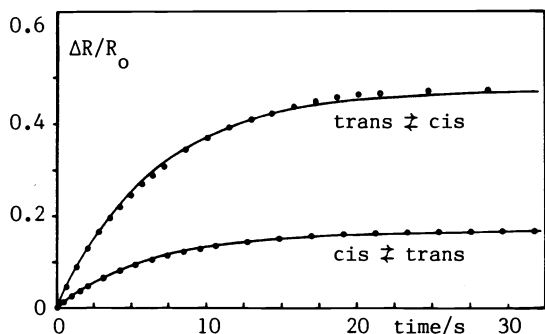


Fig. 3. Photoisomerization of trans- and cis-azobenzene adsorbed from n-hexane on alumina (0.2 mg/g, $T_a = 100^\circ\text{C}$) investigated by change of reflectance. Trans-AB was irradiated and monitored in the S_2 -band, cis-AB in the S_1 -band. Curves are calculated with $\sigma = 200\text{ cm}^{-1}$ and quantum yields of Table 2. Points are measured.
 $I_0 = 4 \cdot 10^{-9}\text{ Einst cm}^{-2}\text{ s}^{-1}$ (Figs. 3. and 4.)

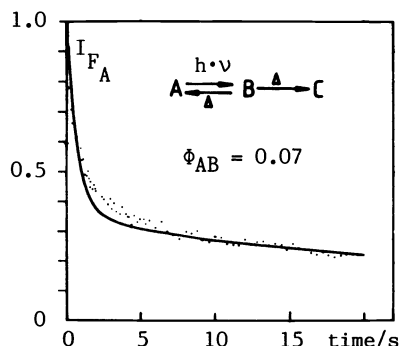


Fig. 4. Photoreduction of acridine adsorbed from n-hexane on titania "Optipur" (0.1 mg/g, no thermal pretreatment) investigated by the fluorescence decrease of acridine. $\nu_{\text{ex}} = 28000\text{ cm}^{-1}$. The curve is calculated with $\sigma = 2000\text{ cm}^{-1}$, $\alpha_{\text{TiO}_2} = 2300\text{ cm}^{-1}$, $\alpha_{\text{AC}} = 86\text{ cm}^{-1}$

LIFETIMES OF PHOTOEXCITED ELECTRONIC STATES

Excited singlet states

The lifetimes of the electronically excited singlets and consequently the photochemical reactivity of the adsorbates can be strongly disturbed by interaction with the electronic system of the adsorbent. It must be distinguished between adsorbents with energy levels close to the levels of the adsorbates (metals, semiconductors, ionic insulators doped with transition metal ions), and adsorbents with energy levels far away from them (main group metal oxides). In the first case, often fast non-radiative deactivation pathways are found via energy or (reversible) charge transfer to the electronic states of the adsorbents. So the fluorescence of many dyes and aromatic hydrocarbons (rhodamine B, fluorescein, pyrene, anthracene) is almost completely quenched on titania, especially after adsorption from HV. Some remaining fluorescence of pyrene, anthracene etc. could be observed by adsorption from aqueous phase (ref. 20), and it seems, that the structure and thickness of the adsorbed water layer is very important for the overlap between the electronic systems of adsorbent and adsorbate. In cases, where the ground and excited singlets of the adsorbates are located in between the energy gap of titania (e.g. acridinium⁺, perylene, tetracene), the fluorescence remains almost unquenched with lifetimes of 40 - 80 % of the dissolved state.

On main group metal oxides like silica and alumina, the fluorescence of adsorbates is more extensively studied and better understood. In principle, the lifetimes are almost the same as in polar solvents, provided that no specific interaction with the surface takes place (CT-complexation, proton transfer, suppression of torsional motions). It is, however, quite common on surfaces that the decay curves are nonexponential (ref. 8-14). Usually this type of decays is explained by superposition of different exponentials arising from molecules adsorbed at different binding sites.

Since almost all types of fluorescent organic molecules show this behavior, the effect seems to be rather unspecific and it is difficult to find a suitable probe molecule which allows to qualify the different nature of the sites more precisely. Perhaps 1,6-diphenyl-hexatriene

(DPH) is such a molecule. Its $S_1 - S_0$ transition is symmetry forbidden and its fluorescence lifetime τ depends very strongly on the $S_2 - S_1$ energy difference. This difference decreases - and parallel to it τ - with increasing polarizability of the environment (ref. 25). In Fig. 5 the decay of DPH on porous alumina and its time-resolved fluorescence spectrum is shown. The long lived component of fluorescence is shifted by 250 cm^{-1} to higher energies and indicates a reduced polarizing environment. As the shift is almost absent on spherical alumina, the high energetic fluorescence is tentatively assigned to DPH adsorbed in pores.

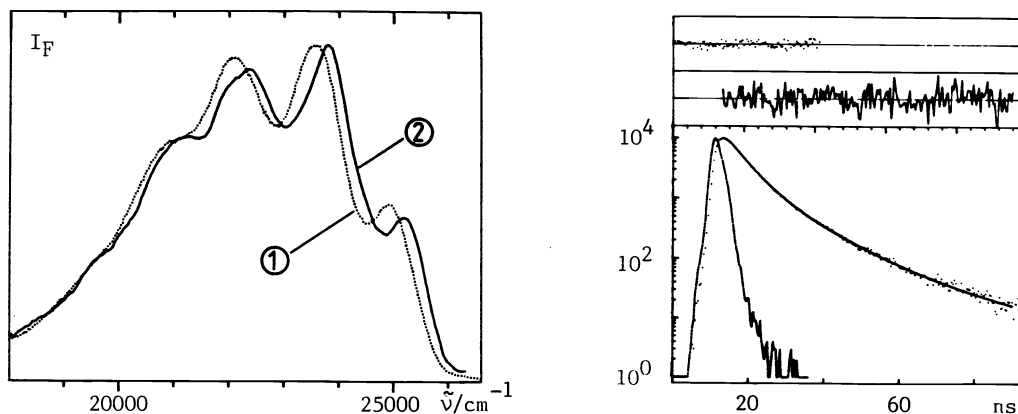


Fig. 5. Fluorescence spectra, 1) steady state, 2) time-resolved, gated after 50 ns, and fluorescence decay of 1,6-diphenylhexatriene on alumina, $T = 50 \text{ K}$. The decay curve is fitted triexponentially with $\tau_1 = 4.5 \text{ ns}$ (58 %), $\tau_2 = 10.5 \text{ ns}$ (35 %), $\tau_3 = 26 \text{ ns}$ (7 %).

Of course, only part of the nonexponential decay can be explained by inner adsorption sites, especially if the long component is about three times longer than the intrinsic lifetime in solution. We have found such decays preferentially on microdisperse aerosols of silica and alumina consisting of small spheres with diameters of 10 to 40 nm and no inner surface. Examples on alumina of adsorbates with fully allowed fluorescence transition and quantum yields ≥ 0.85 in solution are given in Table 1. The concentration of the adsorbates was only ca. 1 molecule per 5 particles of adsorbent in order to exclude aggregation as complete as possible.

TABLE 1. Fluorescence lifetimes of some adsorbates with high fluorescence yields adsorbed on microdisperse alumina

Adsorbate	mean	biexponential fit		values in
	decay time	amplitudes in brackets		solution
	τ/ns	τ/ns	τ/ns	τ/ns
9,10-diphenylanthracene	15	6 (32)	20 (68)	7 - 8
perylene	11	7.5 (47)	14 (53)	6 - 7
fluorescein monoanion	6.5	4.5 (57)	9 (43)	4
stilbene at $T = 50 \text{ K}$	2.7	1.7 (57)	3.9 (43)	1.6

Obviously the short component is almost the same as in solution. The long component is explained as not being mainly due to local inhomogeneities of the surface but by interference between directly emitted radiation and radiation scattered from the microscopic adsorbent. Like in front of a dielectric mirror (ref. 26) the lifetime of the emitter depends strongly on the orientation of the electric dipole transition moment relative to the surface of the particle. The properties of the scatterer affecting the lifetimes are its scattering indicatrix and refractive index relative to the environment. So the long fluorescence component disappears almost completely by adding an inert liquid aliphatic hydrocarbon to the adsorption system which reduces the relative refractive index. It reappears by vacuum evaporation of the solvent at room temperature.

Lifetime components on insulators which are definitely shorter than in solution can be attributed to impurity quenching via energy transfer to acceptor levels in the solid (impurity acceptors in alumina are e.g. iron(III) and chromium(III)) or to enhanced ISC by the external heavy atom effect. We have extensively studied the latter effect on thoria. In principle, the ISC rates are definitely higher than on adsorbents with low nuclear charge. So naphthalene and phenanthrene are strongly phosphorescent and their fluorescence yield is reduced to 10^{-3} . But there are exceptions like perylene and anthracene which are fluorescent with lifetimes and quantum yields close to those on alumina.

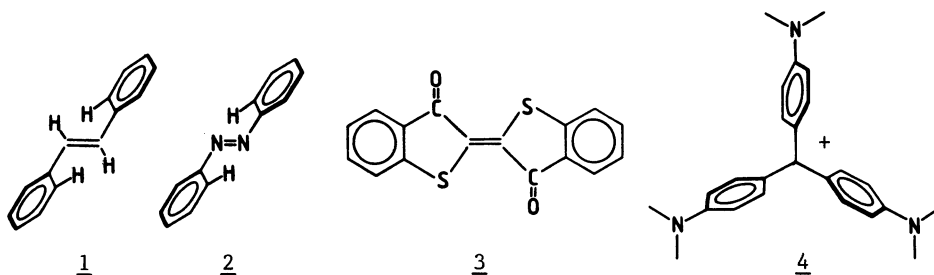
Excited triplet states

One of the most striking luminescence effects of adsorbed aromatics is their intense room-temperature phosphorescence (ref. 27-29). Especially HV-adsorbates on alumina show decay times in the second scale which are still ca. 50 % of the low-temperature values. Thus the long lifetime of triplet states makes them extremely sensitive to photochemical processes. In cases, where the phosphorescence signal is difficult to observe, the decay curves can be monitored by diffuse reflectance triplet-triplet absorption. The results are quite similar to phosphorescence. The lifetimes are much longer than in solution, achieving sometimes the values in rigid solvents at low temperatures. On silica we found e.g. for acridine $\tau = 30$ ms, stilbene $\tau = 3$ μ s, DPH $\tau = 5$ μ s (ref. 30).

INTERNAL MOBILITY OF PHOTOEXCITED ADSORBATES

In general, the mobility of those parts of the adsorbed molecule is reduced, which are in close contact to the surface. The energy of adsorption can be treated like an additional activation barrier of rotation, vibration or translation, provided the reacting part of the molecule has really to be desorbed in the transition state. In many nonplanar molecules this is not necessarily the case. The reacting groups can behave like in vacuum, and the absent viscosity of the environment raises the preexponential factor of the reaction rate constant. On the other hand, it is a severe problem in unimolecular reactions of isolated molecules to transform electronic excitation energy into nuclear motions. The thermal bath of the adsorbent with very low-energetic vibrational levels is by no means an ideal collision partner to induce internal electronic - vibronic transitions. Thus it is very difficult to predict the rate constants of internal motions of adsorbed molecules.

In the following, four examples will be discussed in detail. Three of them are famous candidates for trans-cis photoisomerization in liquid and gas phase, the fourth is a representative of triphenylmethane dyes with strongly viscosity dependent fluorescence yields. Only thioindigo is planar.



trans-cis photoisomerization

The quantum yields of the three compounds (1, 2, 3) adsorbed on alumina are summarized in Table 2. Only trans-thioindigo is absolutely not isomerizable at room temperature, contrary to its behavior in solution and, to some extent, at high surface coverages (ref. 31). The electronic transitions are shifted by more than 2000 cm^{-1} to the red, indicating a strong polarizing interactions of the π - and n -electrons with the surface. Probably the molecule is adsorbed flatly, and it is impossible to rotate it around the central double bond without overcoming its total desorption energy.

Trans-stilbene was used as one of the first molecules to study photoreactions in the adsorbed state (ref. 32-34), and it belongs probably to those organic molecules whose photophysics and photochemistry has been most thoroughly investigated in homogeneous phase. The rate of trans-cis isomerization depends on viscosity and on temperature. It is well accepted that an activation barrier ΔE in the S_1 state is responsible for the temperature dependence of the torsional rate constant $k_{t,p}$ from the trans- to the perpendicular configuration in S_1 . From this configuration the excited molecule deactivates with the probability w to the cis-

and with the probability $(1-w)$ back to the trans-ground state (ref. 35). Using this model, we have calculated the kinetic parameters of adsorbed trans-stilbene by the temperature dependent fluorescence lifetimes τ_F , fluorescence quantum yields η_F and quantum yields of photoisomerization $\phi_{t,c}$. Some of the experimental results and calculated data are given in the Fig. 6 and Table 3.

TABLE 2. Quantum yields of the photochemical trans - cis isomerization at room temperature of some organic molecules adsorbed on alumina.

		on alumina		in liquid solution	
		S_1 -excitation	S_2 -excitation	S_1 -excitation	S_2 -excitation
azobenzene	$\phi_{t,c}$	0.35 ± 0.10	0.20 ± 0.05	0.20 ± 0.05	0.15 ± 0.05
	$\phi_{c,t}$	0.65 ± 0.05	0.55 ± 0.10	0.50 ± 0.10	0.30 ± 0.10
stilbene	$\phi_{t,c}$	0.05 ± 0.02		0.50 ± 0.05	
	$\phi_{c,t}$	0.40 ± 0.10		0.35 ± 0.05	
thioindigo	$\phi_{t,c}$	$\approx 10^{-5}$		0.15 ± 0.05	
	$\phi_{c,t}$	---		0.40 ± 0.10	

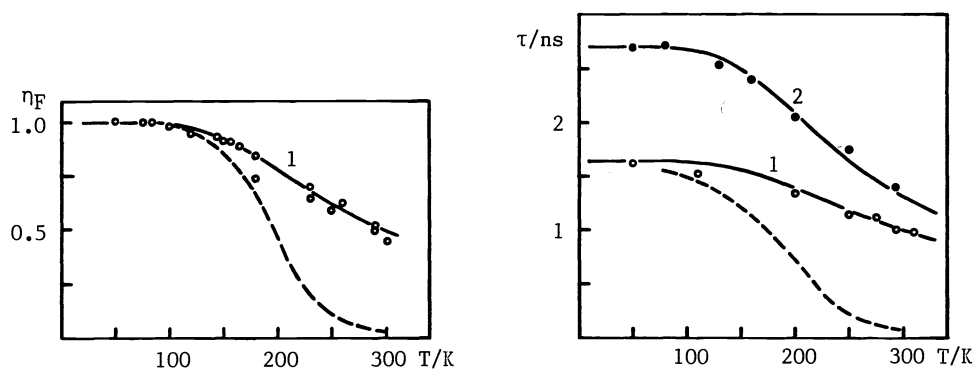


Fig. 6. Temperature dependence of the fluorescence quantum yield and the mean fluorescence lifetime of stilbene on aluminas (adsorbed from HV) and in solution.

Points: Measured on 1) porous alumina 2) microspherical alumina

Dashed lines: Mean values in several solutions

Solid lines: Calculated using the equations and data below

TABLE 3. Kinetic constants of photoexcited stilbene adsorbed on porous alumina and dissolved in low-viscous solvents, $T = 300$ K.

	alumina	solution	
η_F	0.45 ± 0.05	0.06 ± 0.02	$\tau_F^{-1} = k_F^0 + k_{t,p}^\infty \exp(-\Delta E/RT)$
τ_F	1.0 - 1.4 ns	50 - 130 ps	$\eta_F^{-1} = 1 + \tau_F^0 k_{t,p}^\infty \exp(-\Delta E/RT)$
w	0.12 ± 0.05	0.55 ± 0.05	$\phi_{t,c} = w \tau_F k_{t,p}^\infty \exp(-\Delta E/RT)$
ΔE	6 ± 0.5 kJ/mol	8 - 16 kJ/mol	
$k_{t,p}^\infty$	$5 \cdot 10^9 - 8 \cdot 10^9$ s ⁻¹	$10^{12} - 10^{13}$ s ⁻¹	

Obviously the photoisomerization of *trans*-stilbene is reduced in the adsorbed state but not completely suppressed at room-temperature. The reduced mobility in S has to be mainly explained by a lower preexponential factor and not by a higher activation energy for rotation. If ΔE is compared with the adsorption energy of ca. 40 kJ/mol (ref. 33) it can be concluded that part of the molecule has retained its torsional degrees of freedom like in the gas phase. Under this assumption also the low value of $k_{t,p}^{\infty}$ becomes understandable which is much closer to the values of $10^{10} - 10^{11} \text{ s}^{-1}$ in the collisionfree jet stream (ref. 36) than to the values in condensed phase.

Finally, the rate of photoisomerization of adsorbed *trans*-azobenzene is almost the same as in liquid solution. According to the diffuse reflectance spectra (ref. 37) the molecule is strongly H-bonded at one or, as we have shown for the adsorbed *cis*-compound, even at both nitrogen atoms. It is well accepted that azobenzene isomerizes by a mechanism of inversion (ref. 38). This type of motion needs no desorption, neither in the parallel nor in the perpendicular orientation of the π -electronic system relative to the surface plane.

Torsional motions of triphenylmethane dyes

The fluorescence of this type of compounds is strongly viscosity dependent and it is assumed that barrierless or low-barrier torsional twisting of the phenyl rings, accompanied by intramolecular charge transfer (TICT), is the reason for fluorescence quenching (ref. 39,40).

We investigated the cationic dye crystal violet (4) and the neutral dye aurin which is, however, adsorbed on alumina as monoanion and dianion. From our experiences with aromatic bases and acids, both molecules are adsorbed via their functional para-groups and not via their propeller shaped phenyl rings. Under this assumption at least one of the phenyl rings is not in contact with the surface and behaves like in vacuum. At room-temperature the fluorescence yield of the adsorbates is very low, comparable with the low yield in fluid solution. On cooling down, the fluorescence in solution increases dramatically because of the increasing viscosity of the solvent. Contrary to this, the fluorescence of the adsorbate changes only very little within the temperature range in question (see Fig. 7). Even at 50 K no saturation level of the fluorescence is obtained (further cooling is problematic because it needs some contact gas which behaves like an additional medium). The result shows clearly the difference between strongly temperature dependent viscosity and temperature independent or non-existent viscosity, and answers also the question of the torsional barrier in crystal violet: it is indeed very low, much lower than e.g. in photoexcited *trans*-stilbene (Fig. 6, Tab. 3).

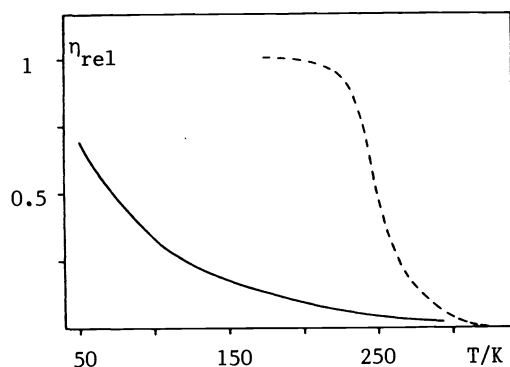


Fig. 7. Fluorescence quantum yield of crystal violet as a function of temperature.

Solid line: adsorbed on alumina, $c = 2 \cdot 10^{-2} \text{ mg/g}$, evacuated sample
Dashed line: dissolved in glycerol data from ref. 40.

Consecutive reactions of *trans*-azobenzene and *trans*-stilbene

In solution, the photoisomerization reactions of both compounds are followed by ring closure to 9,10-diazaphenanthrene and phenanthrene, resp. Ring closure of azobenzene is observed only in acidified solutions. In the adsorbed state it is especially interesting to investigate the corresponding reactions under HV-conditions, i.e. under strict exclusion of molecular oxygen, in order to have a probability as high as possible to stabilize the very reactive dihydro-intermediates.

In the case of adsorbed *trans*-azobenzene a fluorescent consecutive product is formed which we could unambiguously assign to 9,10-diazaphenanthrene by its fluorescence, phosphorescence and excitation spectra (s. Fig. 8). Compared to the *trans*-*cis* yield, the yield of ring closure is very low, but it increases dramatically in the following series:

silica < alumina ($T_a = 100 \text{ }^\circ\text{C}$) < alumina ($T_a = 300 \text{ }^\circ\text{C}$) < silica/alumina mixed oxide.

Assuming the same mechanism of ring closure as in solution, this series reflects impressively the increasing proton-catalytic efficiency of the surfaces. No intermediate dihydro-precursor of azaphenanthrene was found in the spectra or in the kinetics, and it must be

concluded that such intermediates - if they are stable at all - are rapidly oxidized by hydrogen abstraction.

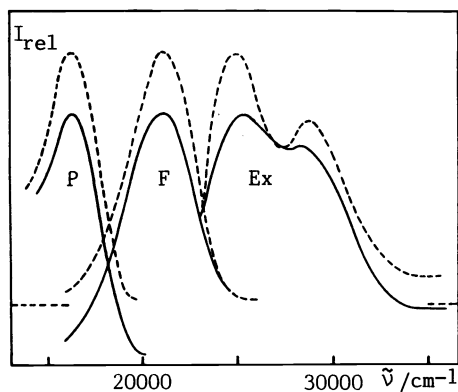


Fig. 8. Fluorescence (F), phosphorescence (P) and fluorescence excitation (Ex) spectra of

Dashed lines:
9,10-diazaphenanthrene/alumina ($T_a = 100\text{ }^\circ\text{C}$)

Solid lines:
azobenzene/alumina ($T = 100\text{ }^\circ\text{C}$)
after 120 m of irradiation at 29000 cm^{-1}
($I_0 = 4 \cdot 10^{-9}\text{ E cm}^{-2}\text{s}^{-1}$, $c = 0.2\text{ mg/g}$)

In the case of adsorbed trans-stilbene only negligible traces of phenanthrene are formed, even after extended alternating irradiation in the regions of maximum trans- and cis-absorption. However, a new fluorescent photoproduct could be detected which is not known from solution. The fluorescence and excitation spectrum of this product is moderately structured, similar to aromatic or long-chained polyenic moleculars. The oscillator strength of the first singlet transition is rather low, with a fluorescence decay time of $\tau = 40\text{ ns}$. The main features of the spectrum are very similar to 4a,4b-dihydrophenanthrene in solution (ref. 41), with one decisive difference: the broad absorption band at low energies is completely absent (Fig. 9).

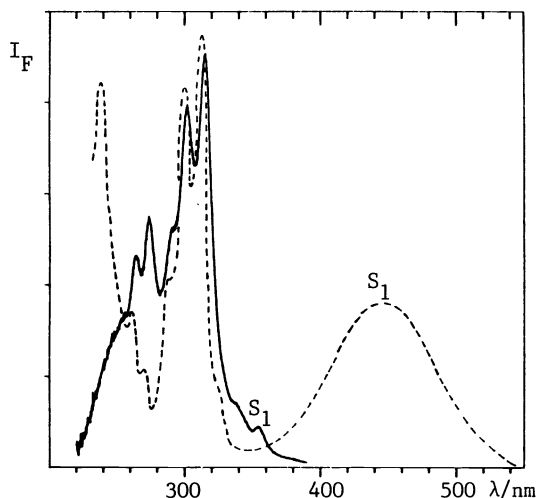


Fig. 9. Solid line: Fluorescence excitation spectrum of the second photoproduct of stilbene adsorbed from HV on alumina ($T_a = 100\text{ }^\circ\text{C}$, $c = 0.1\text{ mg/g}$).

Dashed line: Absorption spectrum of 4a,4b-dihydrophenanthrene in solution (ref. 41).

Nevertheless we assign the spectrum to a product similar to dihydrophenanthrene, since a) the photoreaction is reversible, and b) comparable results are obtained with adsorbed triphenylethene and tetraphenylethene, but not with 1,1-diphenylethene, styrene or phenylpropene. The final identification of the adsorbate is not possible at this stage of investigations.

TRANSLATIONAL MOTIONS OF PHOTOEXCITED ADSORBATES

Bimolecular photoreactions between adsorbed molecules require some lateral mobility of at least one of the reactants. Lateral displacements depend mainly on the activation barrier between adjacent binding sites and on the lifetimes of the excited states. Obviously adsorbents with uniform surface structure, and single-bonded adsorbates with low binding energies are favoured for translational motions.

We have found e.g. aza-aromatics with weakly basic nitrogen atoms to be considerably mobile on fully hydroxylated silica surfaces, to which the molecules are H-bonded via their nitrogen atoms. Contrary to this, no mobility is found on aluminas, to which the molecules are adsorbed as protonated ionic species. The mobility on silica can also be strongly reduced by partial dehydroxylation of the surface, making it impossible to the molecules to move without loosening their H-bonds.

The most detailed information could be obtained by time-resolved triplet-triplet (TT) absorption (ref. 16) and luminescence studies of 9-aza-anthracene (acridine). At room-temperature the fluorescence decay times of the adsorbate, not in contact with a second acridine, are between $\tau_F = 2$ ns and 50 ns, and the triplet decay times are between $\tau_T = 3$ μ s and 30 ms, both depending on the chemical nature of the adsorbate. With increasing coverage of silica the TT absorption decay curve shortens strongly and becomes non-exponential. Parallel to this, an intense delayed fluorescence signal I_d appears after laser-excitation, consisting of two bands which we assign to monomeric H-bonded acridine and to acridine excimers. Intensity and decay time of I_d change strongly with coverage, and the phenomenon of delayed fluorescence disappears totally on highly preheated silica ($T_a = 600$ °C). Our results can be explained almost quantitatively by the following reaction scheme

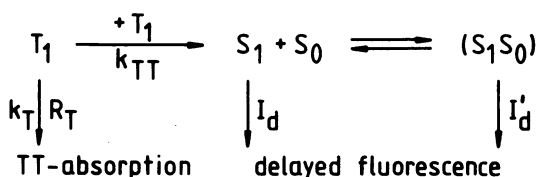


TABLE 4. Acridine/silica. Intensity and decay characteristics of the delayed fluorescence I_d , and TT absorption R_T at room-temperature. Laser excitation 30 mJ/pulse. Initial slopes of the decay curves are given relative to their amplitudes at $t = 0$.

concentration of acridine c (mg/g)	$T_a = 100$ °C			$T_a = 600$ °C ($I_d = 0$)
	I_d	dI_d/dt (s^{-1})	dR_T/dt (s^{-1})	dR_T/dt (s^{-1})
1	1	$2.8 \cdot 10^4$	$1.1 \cdot 10^3$	$3.5 \cdot 10^1$
0.7	0.4	$8 \cdot 10^3$	$5 \cdot 10^2$	
0.1	$< 10^{-2}$	$\approx 10^2$	$4 \cdot 10^1$	$3.5 \cdot 10^1$

The detailed kinetics of deactivation will be given elsewhere (ref. 30). A bimolecular TT annihilation constant of $k_{TT} = 3 \cdot 10^6$ $M^{-1}s^{-1}$ has been calculated on silica ($T_a = 100$ °C) which is only by three orders of magnitude smaller than in fluid solution (ref. 42).

PHOTOINDUCED CHARGE SEPARATION

The first excited species initiating charge transfer can be the adsorbate as well as the adsorbent. It is beyond the scope of this article to enter into the numerous works on the mechanisms of heterogeneous redox reactions following the primary step of electronic excitation. We would like to emphasize only that, with the methods described, we are able to detect short-lived intermediates which are formed with low quantum yields, and to analyze the process of charge separation under free selectable monochromatic irradiation using conventional broad-band light sources and double monochromators.

Very often, charge separation is only a side reaction. Excited aromatic and polyenic hydrocarbons, adsorbed on fully hydrated alumina or silica, are e.g. assumed to deactivate by intramolecular processes exclusively. However, part of the diffuse reflectance flash photolysis spectra of diphenylpolyenes show that the adsorbates are ionized with a quantum yield of ca. 1 % into cation radicals by electron transfer to the solid (ref. 30). Despite of the low quantum yields and the low surface coverages, the absorption signals of the radicals amount to 60 % so that they are easily to be detected. The adsorbed radicals are much longer

lived than in fluid solution. They recombine according to very complex kinetics beginning in the microsecond timescale and ending in the second or even minute timescale.

On photoexcited semiconductors, simultaneous reduction and oxidation of adsorbed species take place. In detail, the reactions depend on the energy of the photoexcited electron-hole pairs, on the probability of pair dissociation, and the migration of the charge carriers to the surface. These processes change with excitation energy, and it is desirable to investigate the reduction and oxidation steps separately under variable wavelengths of irradiation.

Under this aspect the photoadsorption and photodesorption of oxygen on titania will be discussed. The reactions are usually studied under broad-band irradiation, but the steps of desorption (oxidation of surface oxide or hydroxide ions) and adsorption (reduction of gaseous or dissolved oxygen to O_2^- ions) can have different wavelength characteristics. Thus it is difficult under polychromatic irradiation to establish a detailed mechanism of reaction. We succeeded in studying the reaction in ethanolic suspension under monochromatic irradiation using the fluorescence of dissolved perylene as a probe for the oxygen concentration in ethanol. The reaction rates at different wavelengths are given in Fig. 10

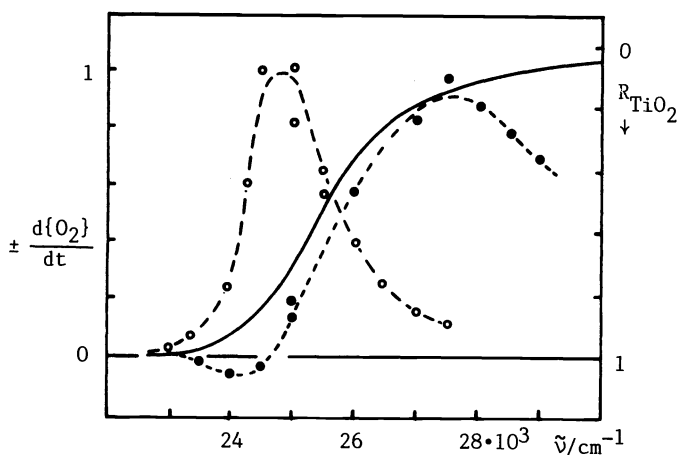


Fig. 10. Initial reaction rates of the photodesorption (open circles) and the photoadsorption (closed circles) of oxygen on microdisperse titania (P25, Degussa) suspended in ethanol versus the wavelength of irradiation. The rates are normalized to equal intensities of irradiation. Negative adsorption rates: at these wavelengths always desorption is found, even in oxygen-saturated solutions. Solid line: Diffuse reflectance spectrum of the adsorbent.

Obviously desorption predominates at band-gap or sub-band gap irradiation. At higher energies of irradiation, the adsorption process becomes more and more important. The maximum quantum yield of desorption $\Phi_{des} = 0.2$ (calculated on the basis of four positive holes per oxygen produced) is much higher than the maximum yield of adsorption $\Phi_{ads} = 0.03$ (calculated on the basis of one photoelectron per oxygen chemisorbed), supporting the experience that titania is a much better oxidizing photocatalyst than a reducing one. However, closer inspection of Fig. 10 clearly shows that this has to be strongly modified with excitation energy.

Acknowledgement

Financial support by the Deutsche Forschungsgemeinschaft, the European Community (contract Nr. STI-016-J-C) and the Fond der Chemischen Industrie is gratefully acknowledged.

REFERENCES

- 1) P.de Mayo, *Pure & Appl. Chem.* **54**, 1623 (1982)
- 2) A.Henglein, *Pure & Appl. Chem.* **56**, 1215 (1984)
- 3) A.J.Nozik (Editor), "Photoeffects at Semiconductor-Electrolyte Interfaces" ACS Symposium Series 146 (1981)

- 4) M.A.Fox (Editor), "Phototransformations in Nonhomogeneous Media"
ACS Symposium Series 278 (1985)
- 5) G.Kortüm, "Diffuse Reflectance Spectroscopy" Springer, Berlin-Heidelberg-New York, (1969)
- 6) D.Oelkrug, M.Radjaipour and H.Erbse, Z.physik.Chem. **88**, 23 (1974)
- 7) D.Oelkrug and M.Radjaipour, Z.physik.Chem. **123**, 163 (1980)
- 8) R.W.Kessler, D.Oelkrug, S.Uhl, Le Vide, les Couches Minces **209**, 1338 (1981)
- 9) R.K.Bauer, R.Borenstein, P.de Mayo, K.Okada, M.Rafalska, W.R.Ware and K.C.Wu,
J.Am.Chem.Soc. **104**, 4635 (1982)
- 10) R.K.Bauer, P.de Mayo, W.R.Ware and K.C.Wu, J.Phys.Chem. **86**, 3781 (1982)
- 11) D.R.James, Y-S.Liu, P.de Mayo and W.R.Ware, Chem.Phys.Lett. **120**, 460 (1985)
D.R.James and W.R.Ware, Chem.Phys.Lett. **120**, 450 (1985)
- 12) D.Avnir, R.Busse, M.Ottolenghi, E.Wellner and K.A.Zachariasse, J.Phys.Chem. **89**, 3521 (1985)
- 13) R.W.Kessler, S.Uhl, W.Honnen and D.Oelkrug, J.Luminesc. **24/25**, 551 (1981)
- 14) S.Uhl, G.Krabichler, K.Rempfer and D.Oelkrug, J.Mol.Struct. **143**, 279 (1986)
- 15) R.W. Kessler and F.Wilkinson, J.C.S.Faraday Trans.I **77**, 309 (1981)
- 16) F.Wilkinson and C.J.Willsher, Chem.Phys.Lett. **104**, 272 (1984)
- 17) G.Beck and J.K.Thomas, Chem.Phys.Lett. **94**, 553 (1983)
- 18) K.Rempfer, S.Uhl and D.Oelkrug, J.Mol.Struct. **114**, 225 (1984)
- 19) D.Oelkrug, H.Erbse and M.Plauschinat, Z.physik.Chem. **96**, 283 (1975)
- 20) K.Chandrasekaran and J.K.Thomas, J.Am.Chem.Soc. **105**, 6383 (1983);
J.Coll.Int.Sci. **106**, 532 (1985)
- 21) E.Wellner, M.Ottolenghi, D.Avnir and D.Huppert, Langmuir (1986), in press
- 22) W.Honnen, G.Krabichler, S.Uhl and D.Oelkrug, J.Phys.Chem. **87**, 4872 (1983)
- 23) S.Chandrasekhar, "Radiative Transfer", Clarendon Press, Oxford, 1950
- 24) P.Kubelka and F.Munk, Z.Tech.Phys. **12**, 593 (1931); P.Kubelka, J.Opt.Soc.Am. **38**, 448 (1948)
- 25) E.D.Cehelnik, R.B.Cundall, J.R.Lockwood and T.F.Palmer, Chem.Phys.Lett. **27**, 568 (1974)
- 26) K.H.Drexhage, in E.Wolf(Ed.), "Progress in Optics XII", 163, North Holland, Amsterdam, 1974
- 27) E.M.Schulman and C.Walling, J.Phys.Chem. **77**, 902 (1973)
- 28) D.Oelkrug, M.Plauschinat and R.W.Kessler, J.Luminesc. **18/19**, 434 (1979)
- 29) R.A.Dalterio and R.J.Hurtubise, Anal.Chem. **54**, 224, (1982)
- 30) D.Oelkrug, G.Krabichler, S.Uhl, F.Wilkinson and C.J.Willsher, in prep.
- 31) H.D. Breuer and H.Jacobs, Chem.Phys.Lett. **73**, 172 (1980)
- 32) L.D.Weis, T.R.Evans and P.A.Leermakers, J.Am.Chem.Soc. **90**, 6109 (1968)
- 33) H.Moesta, Disc.Faraday Soc. **58**, 244 (1974)
- 34) G.H.Hecht and J.L.Jensen, J.Photochem. **9**, 33 (1978)
- 35) G.Orlandi and W.Siebrand, Chem.Phys.Lett. **38**, 352 (1976)
- 36) A.Amirav and J.Jortner, Chem.Phys.Lett. **95**, 295 (1983)
- 37) H.Rau, Ber.Bunsenges.Phys.Chem. **75**, 1347 (1971)
- 38) H.Rau and E.Lüddeke, J.Am.Chem.Soc. **104**, 1616 (1982)
- 39) D.Ben-Amotz and C.B.Harris, Chem.Phys.Lett. **119**, 305 (1985)
- 40) M.Vogel and W.Rettig, Ber.Bunsenges.Phys.Chem. **89**, 962 (1985)
- 41) K.A.Muszkat and E.Fischer, J.Chem.Soc.(B) **1967**, 662
- 42) Y.Nishida, K.Kikuchi and H.Kokubun, J.Photochem. **13**, 75 (1980)